Supplementary Materials

David Reens,* Hao Wu,* Tim Langen,† and Jun Ye
JILA, National Institute of Standards and Technology and the University of Colorado and Department of Physics, University of Colorado, Boulder, Colorado 80309-0440, USA
(Dated: October 17, 2017)

The present study on the role of mixed fields for spin-flip loss evolved out of our continuing investigations into the collisional processes of trapped OH molecules in a magnetic quadrupole trap reported in Refs. [1, 2]. The current investigations have revealed that the spin-flip loss can be substantially enhanced when an electric field is applied to the magnetic trap, and thus an important fraction of the inelastic collisional loss under various electric fields is in fact attributable to spin-flip losses. In Sections A, B we provide further information on the electric field-induced trap loss and evaporative cooling, respectively. In Section C we provide an algebraic derivation of the loss enhancement factor presented in Eqn. 3 of the main text [3].

A. Electric Field-Induced Trap Losses

Ref. [1] introduced the single particle spin-flip loss enhancement process and deconvoluted its effect from the inelastic collisional effect (Appendix A, Ref. [1]). Since that time, new and more systematic experimental observations have prompted improvements to the analysis that was presented there.

Relative to the previous approach, we make the same simplifying assumptions: loss only occurs in the $\vec{E} \perp \vec{B}$ plane, and only the velocity orthogonal to this plane matters as molecules cross this loss plane, and the in-trap population follows a thermalized Maxwell-Boltzmann distribution. Our improvement relates to the next step, where an integral calculation for the loss rate is performed. In Ref. [1] the integration spans the entire 3D spatial distribution, weighted by the frequency of crossing of the center plane and the chance of loss for each crossing:

$$\Gamma_{\mathrm{LZ}} = \int_0^\infty 4\pi r^2\, n(r) dr \int_0^\infty n(v_\theta) dv_\theta \left(\frac{v_\theta}{\pi r} P_{\mathrm{hop}}(r, v_\theta)\right). \quad (1)$$

Here $n(r)$ is the radial distribution function, constrained to satisfy $\int_0^\infty 4\pi r^2 n(r) = 1$, and of the form $n(r) \propto e^{-\mu_B B' r/kT}$. Likewise $n(v_\theta)$ is the usual normalized Maxwellian velocity distribution. Implicit in this integration is the assumption that molecules at a given radius r cross the center plane with a frequency of $v_\theta/\pi r$. This approximation is rather simplistic given that molecules are typically not following circular orbits of constant v_θ but are in general following some complex trap motion.

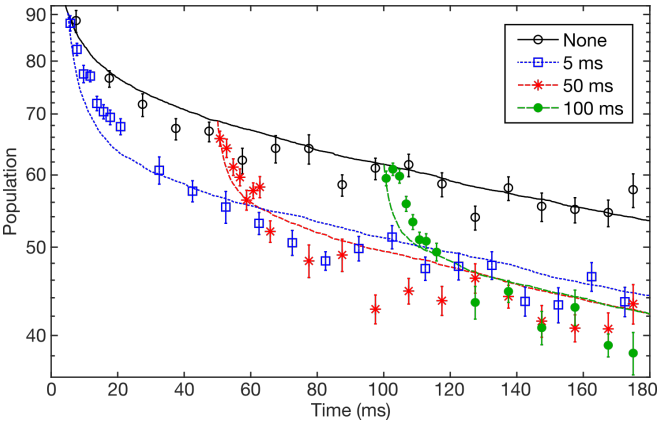

FIG. S1. Experimental data on electric field-induced loss with an attempted overlap to spin-flip loss simulations. The case of no electric field (black, solid, circles) is compared to electric fields of 3 kV/cm turned on after a wait time indicated in the legend.

In addition, the trap is approximated as spherically symmetric to avoid the complication of elliptical coordinates in the three dimension.

A more accurate treatment that we use here is to perform an integration of flux through the loss plane directly:

$$\Gamma_{\mathrm{LZ}} = \int_0^\infty 2\pi r\, n(r) dr \int_0^\infty n(v_z) dv_z \left(v_z P_{\mathrm{hop}}(r, v_z)\right). \quad (2)$$

Here the spatial integration is over the central plane only, hence the $2\pi r$ Jacobean, and the hopping probability is multiplied by v_z to give a flux. The population distribution $n(r)$ is now normalized correctly for an oblate ellipsoidal quadrupole trap, which no longer requires elliptical coordinates since the integration is only in one plane. We change to cylindrical coordinates to highlight our focus on the central plane. This flux integral gives the desired loss rate without any approximations about molecule orbits or plane-crossing frequency. This rigorous treatment provides precisely an overall scaling factor of π relative to the previous estimate. Comparing the integrands and Jacobeans of Eqn. 1 and 2 gives a factor of $\pi/2$, and the change of integration from the spherical trap volume to the loss plane provides a factor of 2 via the distribution $n(r)$.

The influence of this factor on the deconvolution procedure relates to the details of the two-body fitting routine.

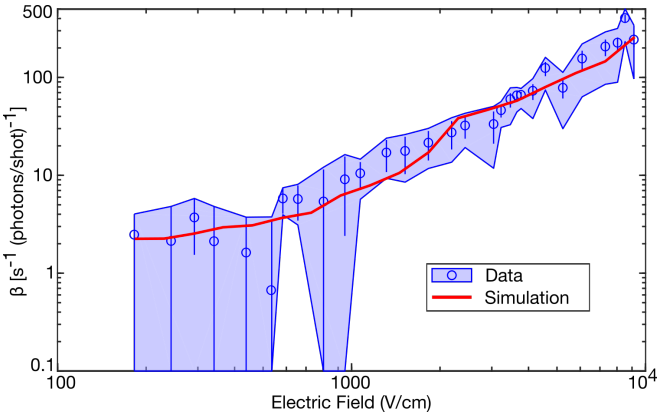

FIG. S2. Two body fits from [1] to experimental data like that in Fig. S1 but at various electric fields. The blue data points and shaded region are repeated from Fig. 3 of [1], where the shading indicates the variation that would be brought about by two-fold changes in γ from spin-flip losses. With a factor of 3 correction noted in this study, the spin flip loss simulation (thick red line) matches the original data within errorbars.

One plus two body fits $\dot{N} = -\gamma N - \beta N^2$ were performed to various decay trap curves, with the one body rate γ fixed to the value expected due to vacuum scattering and spin-flip loss. An example of such decay curves is shown in Fig. S1, where electric field is turned on suddenly after various hold times, which is motivated by the desire to vary the trapped sample density. With the stronger spin-flip loss, we also consider its effect beyond a pure one-body decay. Molecules whose orbits regularly intersect the loss region are lost, after which thermalization would be required to repopulate the loss prone trajectories of phase space. If thermalization is slow, spin-flip loss can have a rate that decreases over time, producing a time dependence of population like that of a two-body effect. Even though the possibility of a factor of two error in the calculated magnitude of spin-flip loss was considered in Ref. [1] (Repeated here in Fig. S2, shaded regions), the possibility of its influencing the data in a non-single-particle manner was not addressed. We note however that both the previous and current derivations of spin-flip loss assume a thermal distribution in the trap.

We have performed single particle Monte Carlo simulations of spin-flip loss to further investigate this effect, and we obtain curves such as shown with the experimental data in Fig. S1. We also performed the same one- plus two-body fitting procedure to the single particle spin-flip loss simulation traces, which yield two-body values that overlap with those derived in Ref. [1], see Fig. S2. This suggests that the spin-flip loss plays an important role in the observed loss data under applied electric fields, and the effect of inelastic collisions is marginal within the errorbars. Still, as we did not involve inelastic collisions in the simulation, there are notable discrepancies between simulation and data, such as in the initial rate of the decays in Fig. S1. One avenue to try and improve agreement would be to incorporate collisions in the simulation. There are many challenges in the quantitative application of these simulations, such as the existence of various partially trapped substates. The best path forward is to perform future collisional experiments with the single-particle effect removed [3].

B. Evaporation

Ref. [2] describes the processes of evaporation from a magnetic quadrupole trap and of depletion spectroscopy to measure the trap distribution. Both processes require two steps. First, molecules are transferred from the positive to the negative parity state by applying short pulses of microwaves tuned to a specific range of magnetic fields. After this transfer, the molecules are still trapped, and only by the subsequent application of a DC electric field to open avoided crossings can these opposite parity molecules escape from the trap. In the case of using depletion spectroscopy for thermometry, the microwave pulses transfer only a small fraction of population between the opposite parity state to reflect the original population distribution [4]. A final step is necessary to measure the overall population in the trap by laser induced fluorescence. The crossings opened by electric field would only allow molecules in the upper 90% of the trap to escape, so it was assumed that a cold population insensitive to the spectroscopic technique would be building up in both parity states at low magnetic fields. Given the existence of spin-flip loss caused by the electric field at the center of the trap where such a cold population would build up, and given its strength for the relevant temperatures and electric fields (Tab. I of the main text [3]), the assumption of cold samples building up in the lower parity state must be reexamined.

Some of the temperature fits performed in Fig. 3 of Ref. [2] relied on this assumption, which we now no longer use. We rely on only the directly experimentally accessible spectra, such as those shown in panels (a-c) (Fig. 3 of Ref. [2]). After taking similar measurements repeatedly, the depletion spectra are found to be useful to identify enhancements in density caused by the evaporation. Figure S3 show such enhancements for evaporation sequences designed to achieve a twofold temperature reduction. The initial temperature of 59 ± 2 mK is higher than reported in Ref. [2], mostly due to a subtle correction to the molecular Hamiltonian. A detailed calculation of this correction including nearly one hundred ground and excited hyperfine levels is given in Ref. [5].

Since depletion spectroscopy transfers only a fraction of molecules to the lower parity state at a specific magnetic field value, we integrate the total area enclosed by the spectroscopy curve, which is scaled according to the observed total population by laser induced fluorescence.

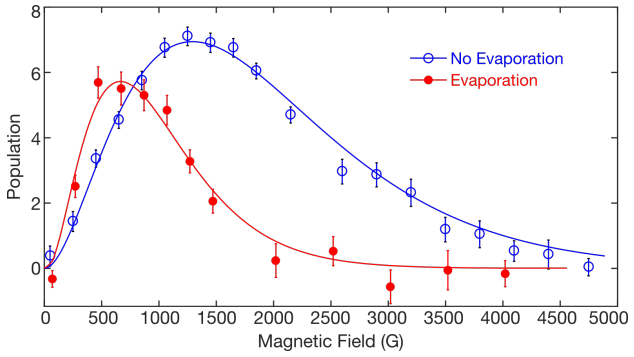

FIG. S3. Depletion spectroscopy spectra are obtained after evaporation (red filled circles) and without evaporation (blue open circles). The integrated areas under the curves correspond to the total number of molecules detected. Solid lines are fits to Maxwell-Boltzmann distributions with temperatures of 59 ± 2 mK without evaporation (blue), and 30 ± 2 mK for evaporation (red). The evaporation achieves a clear density enhancement in the vicinity of 500 G.

This is necessary because depletion spectroscopy is performed with a train of short microwave pulses lasting over a total time of about a quarter of a trap oscillation, so that molecules are not at all frozen in place. Relative to a very brief spectroscopy pulse that would only deplete molecules in a given region at that particular instant, the use of a train of pulses over a longer period of time allows us to sample molecules more widely to boost the signal to noise ratio of spectroscopy. The spectroscopy gives a value that is proportional to the true instantaneous population in a specific magnetic field region, but with a scaling factor that allows the signal to be constrained with the measured total number of molecules in the trap. We carefully include all of the steps in the error analysis leading to the error bars shown in Fig. S3.

In addition to the spatial density enhancement in the low magnetic field region, we can also examine the phase space density (PSD) in the trap, under the assumption of good thermal equilibrium. As the population N was reduced by 60% after evaporation, the temperature came down by a factor of 2. For a quadrupole trap $\mathrm{PSD} \propto N\,T^{-9/2}$, which gives a PSD increase of a factor of 10. It is possible for truncation effects to explain a fraction of this effect. When we perform Maxwell-Boltzmann fits to truncated distribution models, we can see PSD enhancements of at most 6, at which point the truncated models no longer bear much resemblance to a thermal distribution and cannot be fit.

We have also performed another independent verification of the collisional effect by comparing the populations under two closely related experimental sequences. The first is a normal evaporation sequence and the second is identical but with a time-reversed microwave frequency chirp, so that the population cut goes backwards from deep to shallow in the trap. This comparison subjects all molecules to the same integrated microwave power, and thus the two conditions should be equivalent in a situation with only single particle effects. With respect to collisional effects, the time-reversed case functions like a truncation, preventing molecules that would otherwise have collisionally thermalized to lower temperatures from doing so. To whatever extent an evaporation is successful in facilitating beneficial thermalizing collisions, the time-reversed condition should yield fewer molecules. We consistently observe this at the $(6 \pm 2)\%$ level, pointing to an evaporative effect despite the negative influence of spin-flip losses. We have also experimentally observed that under less ideal initial conditions, such as higher initial temperatures of 80 mK resulting from poorer decelerator performance, the density enhancements at low magnetic field and the forward backward differences both disappear, confirming the role of evaporation.

In future work we plan to use a newly developed capability of reducing the population without perturbing its phase space distribution, as reported in the main text [3]. This ought to reduce the influence of collisional processes, but keep any single particle effects the same, thus disambiguating the two. Many possible approaches have key drawbacks, for example changing the partial pressure of water in our supersonic expansion would require changing the temperature of the valve and thereby influencing the initial speed of the beam. We opt for the application of microwaves during deceleration, leading to a probability for transitioning from a weak to strong field seeking state and being deflected out of the beam. We tune the microwaves to be resonant only at low magnitudes of electric fields, experienced by all molecules when flying through a de-energized stage just after switching. The microwaves are applied via horn and have a 17 cm wavelength, so that microwave power variations across the cloud are minimal. The microwaves are applied early during deceleration, so that the molecules have many stages of deceleration left to remix any outstanding asymmetries in the removal process. It is difficult to experimentally verify that the phase space distribution is truly unaffected, but in one projection of phase space, the time of flight profile of slowed molecules after deceleration, the distribution seems to be unaffected even by tenfold reductions using this technique.

While the role of collisional effects in Ref. [2] is reduced by spin-flip losses, especially at low temperatures below 10 mK, spectroscopic comparisons and evaporation subtractions confirm the evaporative effect. The development of forward to backward comparisons and homogeneous density variations will allow us to further distinguish collisional effects from single particle dynamics in the next generation system.